

Hemifusion of Giant Lipid Vesicles Induced by a Small Transient Osmotic Depletion Force

Chang-chun Lee, Shuo Qian, Yen Sun and Huey W. Huang*

Department of Physics & Astronomy, Rice University, Houston, Texas 77251

*Address reprint request to Dr. Huey W. Huang, Department of Physics & Astronomy, Rice University, Houston, Texas 77251-1892. Tel:713 3484899; Fax: 713 3484150; Email: hwhuang@rice.edu

Running title: hemifusion of GUVs by osmotic attraction

Key words: hemifusogenicity, stalk, hemifusion diaphragm, osmotic depletion attraction,

Abstract

We observed hemifusion of giant unilamellar vesicles (GUVs) by injecting a small volume of 5% polyethylene glycol solution in the vicinity for a short time. The induced transient osmotic depletion attraction between two bilayers was smaller than the corresponding van der Waals force, yet hemifusion readily occurred for some lipid compositions. This might imply that the energy barrier for hemifusion is very low if the lipid compositions were primed for the reaction. The barrier for hemifusion is then the task of bringing two membranes into contact. We found that hemifusion is a stochastic event very much like pore formation by tension or by pore-forming peptides. This method provides an operational definition for hemifusogenicity which so far has been defined only qualitatively. Surprisingly the configuration of hemifusion depends on the lipid composition, ranging from a stalk-like hemifusion to a large hemifusion diaphragm. The formation of a large hemifusion diaphragm requires trans-bilayer lipid mixing in the participating GUVs. We also found that hemifusogenicity correlates with the water activity for the stalk phase in the lipid water mixture. The effect of cholesterol on hemifusogenicity was clearly demonstrated.

Because a cell and its organelles are each surrounded by a lipid membrane, a great deal of inter- and intra-cellular molecular redistributions involves membrane fusion or its reverse process. Membrane fusions occurring in different functions, such as fertilization, development, carcinogenesis, viral infection, exocytosis, protein trafficking, mitochondrial remodeling and many others (1-5), are controlled by different proteins (see reviews (6-11)). This is understandable because different functions must be initiated by different signals that require different proteins to respond. Nevertheless an increasing body of evidence suggests common features of lipidic configurations shared by different fusion reactions (6, 7, 11). One important common feature is that all fusions go through an intermediate state called hemifusion (5, 6, 11-15), in which the two outer leaflets of apposed bilayers merge but the two aqueous compartments remain separated by a bilayer formed by the two inner leaflets. Not only does SNARE-mediated fusion transition through a hemifusion intermediate, this intermediate may be used mechanistically to increase the speed of fusion in response to calcium during synaptic transmission (16). Indeed it has been proposed that exocytotic vesicles might be held at the plasma membrane in a ready-to-go hemifusion state to accelerate the completion of fusion upon a triggering signal (17, 18). Thus the formation of hemifusion may be viewed as the first, simpler half of a fusion process.

In this paper we studied how hemifusion occurred between two giant unilamellar vesicles (GUVs) without proteins. We found that hemifusion readily occurred by applying a small, transient osmotic depletion pressure to two closely positioned GUVs, provided the vesicles were made of hemifusogenic lipid compositions. The hemifusogenicity was inversely correlated with the osmotic pressure required to produce a stalk phase (19) in that lipid composition. This provides a quantitative measure of hemifusogenicity. This quality of lipid has so far been characterized based on its spontaneous curvature (6). There is now evidence that although membrane fusion is conducted by the action of proteins, the lipid compositions of the participating lipid bilayers are primed for the event. A recent experiment found an increased concentration of high-curvature lipids in the membrane regions between fusing *Tetrahymena* (20). Given the complexity of a membrane fusion reaction, it is helpful to understand the energy barriers for the various steps a fusion event has to traverse. Our experiment aims to understand the energy barrier for hemifusion by lipid bilayers.

Fusion and hemifusion between GUVs have been studied by many investigators to probe various issues. Different methods used to activate fusion might have given different results. MacDonald and collaborators (21, 22) studied fusion between GUVs of oppositely charged lipids, by fluorescence microscopy. Chanturiya et al. (23) studied electrofusion between a GUV and a planar bilayer by simultaneously monitoring three different markers i.e., lipid dye, aqueous dye and ion conductance. Haluska et al (24) studied how the fusion pore expanded in electrofusion at 50 μ s resolution. Cribier and collaborators (25, 26) studied hemifusion between nucleoside-labeled lipids--with one GUV containing ~5% thymidine-labeled lipid and another containing ~5% adenosine-labeled lipids. In our study we injected a small amount of solution containing 5% polyethylene glycol (PEG) in the vicinity of two closely positioned GUVs. This method led

to a stable hemifusion intermediate. Not only the propensity of hemifusion but also the configuration of the hemifused state (the size of the hemifusion diaphragm) depend on lipid compositions.

Fusion and hemifusion of protein-free lipid vesicles in PEG solutions have been demonstrated since the 80's [for example, (27-31)] and, more recently, were very extensively studied by Lentz and collaborators (32-38). These studies were carried out by measuring the collective responses from suspensions of lipid vesicles. Since fusion and hemifusion are stochastic events, the kinetics observed in individual GUVs are different from the kinetics measured from a suspension.

EXPERIMENT

Materials

1,2-dioleoyl-*sn*-glycero-3-phosphocholine (DOPC), 1,2-dioleoyl-*sn*-glycero-3-phosphoethanolamine (DOPE), cholesterol, and 1,2-dioleoyl-*sn*-glycero-3-phosphoethanolamine-N-(lissamine rhodamine B sulfonyl) (abbreviated as Rh-DOPE) were purchased from Avanti Polar Lipids (Alabaster, AL). High purity calcein was purchased from Invitrogen (Carlsbad, CA), Polyethylene glycol (PEG) of various molecule weights were purchased from Sigma-Aldrich (St. Louis, MO). All materials were used as delivered.

Giant unilamellar vesicles (GUVs)

Two types of GUVs, one with dyes and another without dyes, were produced in 155 mM sucrose solution by the electroformation method (39). For GUVs with dyes, lipids of selected composition and 1% molar ratio of Rh-DOPE were co-dissolved in chloroform. For GUVs without dyes, the same lipid composition without the dye lipid was used. The lipid solution was deposited onto two platinum electrodes. After drying under vacuum, the electrodes were placed 5 mm apart in a chamber filled with 155 mM sucrose solution. For some experiments, an 8 μ M calcein was added to the sucrose solution for the GUVs containing lipid dye. Then 1.5 V AC at frequency 10Hz was applied across the electrodes for 10 minutes. Subsequently the voltage was changed to 3V and the frequency was adjusted to 10 Hz for 40 min, followed by 3 Hz, 15 min; 1 Hz 10 min; and 0.5 Hz 30min. This electroformation method has been shown to produce unilamellar large vesicles (39). The vesicle suspension was then gently collected in a glass vial. The vesicles were used within 24 hrs of production.

Observation chamber

The observation chamber contained 500 μ L of 150 mM glucose solution. The osmolality of every solution used in the GUV experiment was measured by a Wescor Model 5520 dew-point Osmometer (Wescor, Logan, UT). All processes were recorded by a Nikon NS-5 MC camera (Nikon, Tokyo, Japan) for further analysis.

Three micropipettes made by micropipette puller Sutter Instrument Company P-97 (Novato, CA) and refined by microforge Narishige MF-900 (East Meadow, NY), were used in this experiment (see schematic Figure 1A). Pipette 1 (diameter 8-12 μ m) was used to inject a 5% (v/v) PEG 400 solution which had a measured osmolality of 150 mM, the same as the glucose solution in the observation chamber. The micropipette was connected to an electrical

microinjector, Narishige IM-31 (East Meadow, NY), which was driven by a compressed gas tank. A small negative pressure was maintained before and after injection so as to ensure that no PEG solution was leaked. The injection was triggered by a foot switch connected the electrical microinjector set at ~ 1 kPa. The injection rate was estimated as follows. Under the experimental condition, the PEG solution was injected for 20 minutes. By measuring the volume decrease within the injection micropipette ($\sim 18\mu\text{L}$), the injection rate was calculated to be $0.015\mu\text{L}$ per sec.

Micropipette 2 and 3 (diameter 8-16 μm) were used to aspirate and manipulate GUVs. Each was held by a motor-driven micromanipulators Narishige MM-188NE (East Meadow, NY) and connected to a pressure control syringe. The latter was used to create a negative pressure inside the micropipette (40, 41). A double pipette holder, Narishige HD-21 (East Meadow, NY) was used to hold micropipette 1 and 2 on one side, and another pipette holder held micropipette 3 on another side. Their relative positions were adjustable.

Before use, the micropipettes were coated with 1% bovine serum albumin in order to neutralize the charge on the bare glass surface (42) and then washed extensively with 150 mM glucose solution. Similar treatments were applied to the walls of the observation chamber. All GUV experiments were performed at room temperature $\sim 25^\circ\text{C}$.

Experimental procedure

For each run of experiment, $2.5\mu\text{L}$ of a dye-containing GUV suspension and $2.5\mu\text{L}$ of a no-dye GUV suspension (otherwise both made from the same lipid composition) were injected into the observation chamber containing $500\mu\text{L}$ of 150 mM glucose solution. The refractive index contrast between the sucrose solution inside and the glucose solution outside of the GUVs made the vesicles visible without exciting the dye. Two GUVs (one with dye, and one without) of diameter 40-80 μm were each slightly aspirated and held by micropipette 2 and 3. The negative pressure in each micropipette was held constant so that the membrane tension was less than 0.5 dyn/cm (43). The two vesicles were positioned so that they slightly contacted each other. Then, from a distance 150-300 μm , the PEG solution was injected toward the vicinity of the two contacting GUVs. In each run of experiment, the PEG solution was injected until the two GUVs were seen attracted to each other and both GUVs were visibly deflated, then the injection was stopped. The injection time ranged from several seconds to over two hundred seconds, and it varied from run to run even for the GUVs of the same lipid composition. Because the refractive index difference between the pure glucose solution and the PEG solution, the injection was visible under white light.

It is important to note that if the PEG injection had any effect on the GUVs, the effect occurred only during the injection. Once the injection stopped, the PEG molecules were diluted and the bulk effect was negligible. This is shown as follows. The longest time of injection for a successful hemifusion was 250 seconds. Therefore the maximum amount of 5% PEG solution injected into the observation chamber was $3.75\mu\text{L}$. Since the chamber contained $500\mu\text{L}$ of glucose solution, this amounted to a maximum concentration of 0.038% PEG. The PEG induced osmotic depletion attraction between lipid bilayers was carefully measured by Kuhl et al (44). Below 0.1% PEG concentration, there was no detectable effect of osmotic depletion

attraction. Therefore in our experiment the osmotic depletion attraction between the two GUVs was a transient effect during the injection.

After the injection of PEG solution stopped, two possible consequences followed. One possible consequence was that the two GUVs remained adhered to each other. Another possible consequence was that the two GUVs bounced back from deflation and separated from each other (see Movies S1, S2, S3 and movie Captions S1 in Supplementary Material). We monitored the lipid dye transfer between the two GUVs by the fluorescence image recorded throughout the experiment. White light was turned on for short intervals to record the start and the stop of the PEG injection and also to view GUVs if necessary. We defined hemifusion by the presence of lipid dye transfer when the two GUVs adhered to each other.

Content mixing experiment

No fusion was observed in our experiment—none of the two contacting GUVs merged into one. However, to be sure that there was no content mixing between the two aqueous compartments, we included 8 μM calcein (which is below the quenching concentration) in the content of one GUV (with lipid dye). To reduce the background signal due to the small amount of calcein introduced into the observation chamber, a larger observation chamber (2-3mL) was used. We performed this experiment three times with the most hemifusogenic lipid composition, i.e., DOPC/DOPE/cholesterol in 4/4/2 molar ratios. Hemifusion was the result of every run. Lipid dye transfer was observed each time, but no leakage of calcein from its compartment was observed—no content mixing. (Figure 1B)

Turbulent jet and osmotic depletion attraction

The injection of a PEG solution into a body of still solution created a turbulent jet. The video image showed a turbulent region in a cone of an opening angle $\sim 50^\circ$. (The visible turbulent region was short of reaching the GUVs.) According to the theory of turbulence (45), the flow was principally along the axis of the cone. Outside the turbulent region there was a laminar flow. The fluid steadily flowed into the turbulent region through the boundary. Thus the amount of fluid which passed per unit time through the cross section of the cone, Q , increased with the distance x measured from the opening of the micropipette along the axis of the cone. If the amount of fluid emitted from the micropipette per unit time was Q_0 . The theory gave $Q/Q_0 = 1.5 x/a$, where a is the radius of the pipette opening (45). In a typical experiment, $a \sim 4\text{-}6 \mu\text{m}$, and the distance of the GUVs to the pipette was $x \sim 200 \mu\text{m}$. By this order of magnitude estimation, the concentration of PEG in the vicinity of the GUVs was about 0.1%. According to the measurement by a very sensitive surface force apparatus (44), the PEG induced osmotic depletion attraction force at 1% concentration was 1/5 of the corresponding van der Waals attraction between two DMPC bilayers in pure water; the two forces are about equal at 5% PEG concentration. Thus even if we allow an order of magnitude error in the above estimate, the osmotic depletion attraction induced by the PEG injection is very small indeed.

X-ray diffraction

The method of X-ray diffraction to investigate lipid phases was described in detail previously (46, 47). Briefly each lipid composition used in the GUV experiment was deposited

from an organic solution on a thoroughly cleaned Si wafer. The lipid amount was about $0.75\text{mg}/\text{cm}^2$. The organic solvent was a trifluoroethanol (TFE)-chloroform mixture. The ratio of TFE to chloroform was varied to give a uniform spreading on the substrate (48). The organic solvent was then removed in vacuum. Afterwards the deposit was hydrated with saturated water vapor at room or higher ($\sim 35^\circ\text{C}$) temperature. During the measurement, the sample was housed in a temperature-humidity chamber described in (47).

X-ray diffraction was performed with a point source of Cu K_α radiation (operating at $35\text{mA}/40\text{ kV}$), which was first Ni filtered and then focused by a pair of spherically bent x-ray mirrors (Charles Supper Co., Natick, MA). The mirrors were Ni-coated to further reduce the K_β radiation. The X-ray was diffracted off the sample at a grazing angle ($< 1^\circ$) with respect to the substrate. The diffraction pattern was collected by a CCD camera (Photonic Science Ltd, East Sussex, GB) at the sample-to-detector distance 22.88 cm . The distance was measured using silver behenate (The Gem Dugout, State College, PA) as a calibration standard. An X-ray attenuator (a stack of Ni foils) was used to reduce the intensities of the first few orders of reflection normal to the substrate, so as to avoid saturating the pixels on the CCD detector. The measurement was performed at 25°C , with the relative humidity (RH) inside the sample chamber varied from 100% RH to $\sim 55\%$ RH. Three phases were observed and identified by their diffraction patterns (46, 47): lamellar phase, rhombohedral (stalk) phase and the inverted hexagonal phase.

RESULTS AND DISCUSSION

It is well known that PEG has the effect of inducing depletion attraction between lipid bilayers or between a lipid bilayer and a surface (44, 49). To study this force, Evans and collaborators (49, 50) used one flaccid GUV against one tensed GUV, and let the flaccid GUV deformed and adhered to the spherical surface of the tensed GUV in the presence of PEG solution. Initially we performed hemifusion experiment with slightly flaccid GUVs, but found that, when the PEG solution was injected, the flaccid GUVs tended to adhere to the external edge of the micropipette and rupture. In order to make a clear distinction between adhesion and hemifusion, we used only slightly tensed GUVs. This was achieved by using a 155 mM sucrose solution inside the GUVs. Against the 150 mM glucose solution in the observation chamber, a small osmotic pressure built up in the GUVs resulting in a small surface tension. The GUVs were still easily aspirated by the micropipette with a small negative pressure that created a small protrusion in the pipette.

1. Control Experiment

In the control experiment, the PEG solution was replaced by a pure glucose solution of the same osmolality. The same control experiments were performed on all lipid compositions except for pure DOPC, three times for each composition. The glucose solution was injected for 4-5 minutes to two closely positioned GUVs. No attraction between GUVs was observed. This showed that the attraction by the injection of PEG solution was entirely due to the effect of PEG, excluding the possibility that the attraction was due to the flow of the fluid.

2. Four different lipid compositions

Four different lipid compositions were experimented in this investigation. We will denote the compositions in the molar ratios of DOPC/DOPE/cholesterol. The four lipid compositions were pure DOPC, 8/0/2, 5/5/0, and 4/4/2.

When the GUVs were made of pure DOPC, the two GUVs would not adhere with each other (Figure 2). The injection of PEG solution caused the two GUVs to attract to each other and created a small flattening on each GUV at the contact. But as soon as the injection stopped, the GUVs bounced back (see Movie S1). During the injection, the two mutually attracted GUVs could be separated by micromanipulators. Clearly there was no adhesion between them, and there was no transfer of lipid dye from one to another. The same experiment was repeated 11 times. Only in one run a very small amount of lipid dye transfer was observed after injecting the PEG solution for a prolonged 8-10 minutes (see Lipid dye transfer below).

When the GUVs were made of 8/0/2 composition, the injection of PEG solution caused the two GUVs to attract to each other and created a small flattening. When the injection stopped, the two GUVs remained adhered to each other. Gradually the lipid dye transferred from the dyed GUV to the no-dye GUV, indicating hemifusion (Figure 3A). However, the two GUVs could still be separated intact, if pulled by the micropipettes (see Movie S2). This experiment was repeated eight times. Seven times hemifusion occurred, but in one of the eight runs the transfer of lipid dye was not observed.

When the GUVs were made of either 5/5/0 or 4/4/2, the results were very different from the last two cases. During the injection of the PEG solution, the two GUVs suddenly deflated and adhered (see Movie S3). The injection was then stopped. Gradually the lipid dye spread from the dyed GUV to the no-dye GUV (Figure 3B, 3C). The two GUVs would not separate if pulled by micromanipulators. We repeated this experiment 10 times with 5/5/0 and 12 times with 4/4/2. The same result was obtained every time.

The success rates of hemifusion for four different lipid compositions were compiled in Figure 4. We propose to define the hemifusogenicity of a lipid composition based on its success rate. Obviously the definition can be refined by measuring it over a range of PEG concentrations.

3. Lipid dye transfer

The rate of lipid dye transfer in hemifusion reflects the configuration of the hemifusion state (Figure 5). The fluorescence intensity through the dyed GUV (averaged over an area near the center of the GUV) minus the background (averaged over a typical area outside the GUVs) was I_0 . The fluorescence intensity through the originally no-dye GUV minus the background was I . The ratio I/I_0 was measured as a function of time. A number of runs were recorded longer than 5 minutes. The dye transfer curves of some of those long-run records are shown in Figure 5. The I for all DOPC experiments were zero, except for one case mentioned above. The transfer rate for this exceptional case of DOPC was very small (included in Figure 5 for comparison). We were not sure this was hemifusion.

4. Configuration of hemifusion

Two types of hemifusion states were seen in our experiment. From the lipid composition 8/0/2, we observed a hemifusion state with a small contact zone. Although the state was stable during the entire observation time of 4 minutes or longer, and the lipid dye transfer continued, this hemifusion state could be reversed to two separate intact GUVs if pulled by micromanipulators (Movie S2).

The other type obtained from 4/4/2 and 5/5/0 lipid compositions was stable in time and stable against pulling by micromanipulators. We had every reason to believe that this was a state called hemifusion diaphragm (6) in which the dividing plane or the septum was a bilayer separating two internal aqueous compartments, and there was a continuous monolayer enveloping the combined GUVs as shown schematically in Figure 6. Our reason for this conclusion was simple. If the dividing plane were two face-to-face parallel bilayers, there was simply no such adhesion force operating once the PEG injection stopped. As we showed in EXPERIMENT the PEG concentration was at most 0.038% once the injection stopped.

Furthermore, we note that in the hemifusion states of 4/4/2 and 5/5/0, the area of the inner monolayer exceeds the area of the outer monolayer at least by 15% and 10%, respectively. Therefore there had to have lipid transfer from the outer leaflets to the inner leaflets in such hemifusion. Indeed a direct proof was found in the dye lipid transfer. If there were no trans-bilayer lipid mixing, the dye lipid transfer I/I_0 should have saturated at a value $\sim 1/3$. This was explicitly shown by the experiments of Cribier & collaborators (25, 26) who studied hemifusion between nucleoside-labeled lipids. In their case, the contact zone was small, and the lipid dye transfer I/I_0 saturated at a value $\sim 1/3$. As we see in Figure 5, all the examples of dye lipid transfer I/I_0 obtained from 4/4/2 and 5/5/0 exceeded $1/3$. The fact that I/I_0 of different runs saturated at different values seemed to indicate that the degree of trans-bilayer lipid mixing varied for each run.

One of the most interesting findings from our experiments is the dependence of the configuration of hemifusion on the lipid composition. Hemifusion of each lipid composition appeared to produce a characteristic degree of flattening of GUVs (defined as h/R —see Figure 6). The 4/4/2 composition produced the largest hemifusion diaphragm with $h/R \sim 1/3$. The 5/5/0 composition produced a somewhat smaller hemifusion diagram with $h/R \sim 1/5$. The hemifusion state of 8/0/2 composition seemed to have little flattening with $h/R \sim 0$.

These differences in the hemifusion configuration were also reflected in the transfer rate of lipid dye. The larger the hemifusion diaphragm is, the larger the contact rim between the two outer monolayers. Hence the lipid transfer rate is highest for the 4/4/2 composition and slightly lower for 5/5/0 composition, but both are fast compared with the very small rate for 8/0/2 composition.

5. Rhombohedral phase of lipid compositions

The lipids were first prepared in a fully hydrated lamellar phase, a stack of parallel bilayers equally spaced by water layers. When osmotic pressure was applied to the system, water was partially removed and point contacts between bilayers occurred by fluctuations. The two apposed monolayers merged at the contact point and developed into an hourglass-like inter-

bilayer structure called a stalk (19, 47). This was discovered because at sufficiently high osmotic pressure, stalk structures were developed at numerous points of inter-bilayer contacts throughout the stack of bilayers and resulted in a rhombohedral lattice with each unit cell containing a stalk. The structure was resolved by X-ray diffraction (19), which confirmed and validated the long speculated structure as the precursor of membrane fusion (6, 51).

It is reasonable to assume that the hemifusion state formed between two bilayers started with a stalk at an inter-bilayer contact. In fact the hemifusion state for the 8/0/2 composition could be very close to a stalk. Thus we compared the hemifusogenicity of a lipid compositions measured by the success rate of GUV experiment with the water activity (the relative humidity) at which the rhombohedral (stalk) phase of the lipid composition appeared (Figure 7). Not surprisingly there was a strong correlation between the two—the more hemifusogenic the lipid composition is, the higher the water activity for the stalk phase.

CONCLUSION

We have used a very small osmotic depletion attraction force, smaller than the corresponding van der Waals force (44), to induce hemifusion of GUVs. It is worth investigating if such a force can be induced by cellular biomolecules. The initiation of hemifusion is considered a high energy barrier for fusion (6, 11). Based on the result of our experiment, this barrier is mainly the task of bringing two membranes close to each other. Hemifusion under such a condition occurred at random times, indicating that it is a stochastic event, very much like pore formation under tension (52, 53) or by antimicrobial peptides (40, 54). This stochastic nature would not be revealed by the measurements using a suspension of lipid vesicles. For instance, if the rate of lipid dye transfer were measured in a vesicle suspension, it would be the convolution of the rate of transfer in individual GUVs, as measured here (Figure 5), and the rate of stochastic hemifusion events. What determines the stochastic time intervals is unknown.

We believe that our method provides an operational definition for hemifusogenicity, and the definition can be fine-tuned by using a range of PEG concentrations in the injected solutions. Until now the hemifusogenicity of a lipid has been defined qualitatively based on its spontaneous curvature (6). The strong correlation between the hemifusogenicity measured by GUVs and the water activity for the stalk phase measured by X-ray diffraction has two implications. It supports the hypothesis that a stalk is a precursor to a hemifusion diaphragm. It also suggests a more convenient measurement of hemifusogenicity by an equilibrium (X-ray diffraction), rather than a kinetic, experiment. The disparity between the small osmotic pressure used for GUV hemifusion and the large osmotic pressure used to reach the rhombohedral phase is perhaps understandable. The hemifusion of GUVs required only one stalk, but a macroscopic number of stalks were created in the rhombohedral phase.

The most surprising result from this experiment is that the configuration of hemifusion strongly depends on the lipid composition, particularly the effect of cholesterol. Pure DOPC would not undergo hemifusion. However, DOPC with 20% cholesterol produced a stable hemifusion state close to a stalk structure, such that the two GUVs could be mechanically

separated. For highly hemifusogenic lipid compositions, such as 4/4/2 or 5/5/0 in DOPC/DOPE/cholesterol ratios, hemifusion resulted in a large diaphragm. The transformation to such a hemifusion diaphragm required the participating GUV to undergo trans-bilayer lipid mixing. Clearly the effects of cholesterol and other lipid components deserve further investigations.

ACKNOWLEDGMENTS

This work was supported by NIH (US) Grants GM55203 and the Robert A. Welch Foundation Grant C-0991

References

1. Chen, E. H., E. Grote, W. Mohler, and A. Vignery. 2007. Cell-cell fusion. *FEBS Lett* 581:2181-2193.
2. Hoppins, S., L. Lackner, and J. Nunnari. 2007. The machines that divide and fuse mitochondria. *Annu Rev Biochem* 76:751-780.
3. Jahn, R., and R. H. Scheller. 2006. SNAREs--engines for membrane fusion. *Nat Rev Mol Cell Biol* 7:631-643.
4. Kielian, M., and F. A. Rey. 2006. Virus membrane-fusion proteins: more than one way to make a hairpin. *Nat Rev Microbiol* 4:67-76.
5. Sapir, A., O. Avinoam, B. Podbilewicz, and L. V. Chernomordik. 2008. Viral and developmental cell fusion mechanisms: conservation and divergence. *Dev Cell* 14:11-21.
6. Chernomordik, L. V., and M. M. Kozlov. 2008. Mechanics of membrane fusion. *Nat Struct Mol Biol* 15:675-683.
7. Jackson, M. B., and E. R. Chapman. 2008. The fusion pores of Ca(2+)-triggered exocytosis. *Nat Struct Mol Biol* 15:684-689.
8. Harrison, S. C. 2008. Viral membrane fusion. *Nat. Struct. Mol. Biol.* 15:690-698.
9. Wickner, W., and R. Schekman. 2008. Membrane fusion. *Nat Struct Mol Biol* 15:658-664.
10. Rizo, J., and C. Rosenmund. 2008. Synaptic vesicle fusion. *Nat Struct Mol Biol* 15:665-674.
11. Martens, S., and H. T. McMahon. 2008. Mechanisms of membrane fusion: disparate players and common principles. *Nat Rev Mol Cell Biol* 9:543-556.
12. Xu, Y., F. Zhang, Z. Su, J. A. McNew, and Y. K. Shin. 2005. Hemifusion in SNARE-mediated membrane fusion. *Nat Struct Mol Biol* 12:417-422.
13. Lu, X., F. Zhang, J. A. McNew, and Y. K. Shin. 2005. Membrane fusion induced by neuronal SNAREs transits through hemifusion. *J Biol Chem* 280:30538-30541.
14. Giraudo, C. G., C. Hu, D. You, A. M. Slovic, E. V. Mosharov, D. Sulzer, T. J. Melia, and J. E. Rothman. 2005. SNAREs can promote complete fusion and hemifusion as alternative outcomes. *J Cell Biol* 170:249-260.
15. Chernomordik, L. V., V. A. Frolov, E. Leikina, P. Bronk, and J. Zimmerberg. 1998. The pathway of membrane fusion catalyzed by influenza hemagglutinin: restriction of lipids, hemifusion, and lipidic fusion pore formation. *J Cell Biol* 140:1369-1382.
16. Schaub, J. R., X. Lu, B. Doneske, Y. K. Shin, and J. A. McNew. 2006. Hemifusion arrest by complexin is relieved by Ca²⁺-synaptotagmin I. *Nat Struct Mol Biol* 13:748-750.
17. Jahn, R., T. Lang, and T. C. Sudhof. 2003. Membrane fusion. *Cell* 112:519-533.
18. Zimmerberg, J., and L. V. Chernomordik. 2005. Neuroscience. Synaptic membranes bend to the will of a neurotoxin. *Science* 310:1626-1627.
19. Yang, L., and H. W. Huang. 2002. Observation of a membrane fusion intermediate structure. *Science* 297:1877-1879.
20. Ostrowski, S. G., C. T. Van Bell, N. Winograd, and A. G. Ewing. 2004. Mass spectrometric imaging of highly curved membranes during *Tetrahymena* mating. *Science* 305:71-73.
21. Lei, G., and R. C. MacDonald. 2003. Lipid bilayer vesicle fusion: intermediates captured by high-speed microfluorescence spectroscopy. *Biophys J* 85:1585-1599.

22. Pantazatos, D. P., and R. C. MacDonald. 1999. Directly observed membrane fusion between oppositely charged phospholipid bilayers. *J Membr Biol* 170:27-38.
23. Chanturiya, A., L. V. Chernomordik, and J. Zimmerberg. 1997. Flickering fusion pores comparable with initial exocytotic pores occur in protein-free phospholipid bilayers. *Proc Natl Acad Sci U S A* 94:14423-14428.
24. Haluska, C. K., K. A. Riske, V. Marchi-Artzner, J. M. Lehn, R. Lipowsky, and R. Dimova. 2006. Time scales of membrane fusion revealed by direct imaging of vesicle fusion with high temporal resolution. *Proc Natl Acad Sci U S A* 103:15841-15846.
25. Heuvingh, J., F. Pincet, and S. Cribier. 2004. Hemifusion and fusion of giant vesicles induced by reduction of inter-membrane distance. *Eur Phys J E Soft Matter* 14:269-276.
26. Rodriguez, N., J. Heuvingh, F. Pincet, and S. Cribier. 2005. Indirect evidence of submicroscopic pores in giant unilamellar [correction of unilamellar] vesicles. *Biochim Biophys Acta* 1724:281-287.
27. Boni, L. T., J. S. Hah, S. W. Hui, P. Mukherjee, J. T. Ho, and C. Y. Jung. 1984. Aggregation and fusion of unilamellar vesicles by poly(ethylene glycol). *Biochim Biophys Acta* 775:409-418.
28. MacDonald, R. I. 1985. Membrane fusion due to dehydration by polyethylene glycol, dextran, or sucrose. *Biochemistry* 24:4058-4066.
29. Yamazaki, M., and T. Ito. 1990. Deformation and instability in membrane structure of phospholipid vesicles caused by osmophobic association: mechanical stress model for the mechanism of poly(ethylene glycol)-induced membrane fusion. *Biochemistry* 29:1309-1314.
30. Bentz, J., D. Alford, J. Cohen, and N. Duzgunes. 1988. La³⁺-induced fusion of phosphatidylserine liposomes. Close approach, intermembrane intermediates, and the electrostatic surface potential. *Biophys J* 53:593-607.
31. Ellens, H., D. P. Siegel, D. Alford, P. L. Yeagle, L. Boni, L. J. Lis, P. J. Quinn, and J. Bentz. 1989. Membrane fusion and inverted phases. *Biochemistry* 28:3692-3703.
32. Lentz, B. R., and J. K. Lee. 1999. Poly(ethylene glycol) (PEG)-mediated fusion between pure lipid bilayers: a mechanism in common with viral fusion and secretory vesicle release? *Mol Membr Biol* 16:279-296.
33. Haque, M. E., A. J. McCoy, J. Glenn, J. Lee, and B. R. Lentz. 2001. Effects of hemagglutinin fusion peptide on poly(ethylene glycol)-mediated fusion of phosphatidylcholine vesicles. *Biochemistry* 40:14243-14251.
34. Haque, M. E., T. J. McIntosh, and B. R. Lentz. 2001. Influence of lipid composition on physical properties and peg-mediated fusion of curved and uncurved model membrane vesicles: "nature's own" fusogenic lipid bilayer. *Biochemistry* 40:4340-4348.
35. Malinin, V. S., P. Frederik, and B. R. Lentz. 2002. Osmotic and curvature stress affect PEG-induced fusion of lipid vesicles but not mixing of their lipids. *Biophys J* 82:2090-2100.
36. Dennison, S. M., N. Greenfield, J. Lenard, and B. R. Lentz. 2002. VSV transmembrane domain (TMD) peptide promotes PEG-mediated fusion of liposomes in a conformationally sensitive fashion. *Biochemistry* 41:14925-14934.
37. Haque, M. E., and B. R. Lentz. 2002. Influence of gp41 fusion peptide on the kinetics of poly(ethylene glycol)-mediated model membrane fusion. *Biochemistry* 41:10866-10876.
38. Haque, M. E., and B. R. Lentz. 2004. Roles of curvature and hydrophobic interstice energy in fusion: studies of lipid perturbant effects. *Biochemistry* 43:3507-3517.

39. Angelova, M. I. 2000. Liposome Electroformation. In *Giant Vesicles*. P. L. Luisi, and P. Walde, editors. John Wiley & Sons, Chichester. pp. 27-36.
40. Lee, M. T., W. C. Hung, F. Y. Chen, and H. W. Huang. 2008. Mechanism and kinetics of pore formation in membranes by water-soluble amphipathic peptides. *Proc Natl Acad Sci U S A* 105:5087-5092.
41. Sun, Y., C. C. Lee, W. C. Hung, F. Y. Chen, M. T. Lee, and H. W. Huang. 2008. The bound states of amphipathic drugs in lipid bilayers: study of curcumin. *Biophys J* 95:2318-2324.
42. Zhelev, D. V., and D. Needham. 1993. Tension-stabilized pores in giant vesicles: determination of pore size and pore line tension. *Biochim Biophys Acta* 1147:89-104.
43. Kwok, R., and E. Evans. 1981. Thermoelasticity of large lecithin bilayer vesicles. *Biophys J* 35:637-652.
44. Kuhl, T., Y. Guo, J. L. Alderfer, A. D. Berman, D. Leckband, J. Isrealachvili, and S. W. Hui. 1996. Direct measurement of polyethylene glycol induced depletion attraction between lipid bilayers. *Langmuir* 12:3003-3014.
45. Landau, L. D., and E. M. Lifshitz. 1959. *Fluid Mechanics*. Pergamon Press, Oxford. pp. 130-136.
46. Yang, L., L. Ding, and H. W. Huang. 2003. New phases of phospholipids and implications to the membrane fusion problem. *Biochemistry* 42:6631-6635.
47. Yang, L., and H. W. Huang. 2003. A rhombohedral phase of lipid containing a membrane fusion intermediate structure. *Biophys J* 84:1808-1817.
48. Ludtke, S., K. He, and H. Huang. 1995. Membrane thinning caused by magainin 2. *Biochemistry* 34:16764-16769.
49. Evans, E., and D. Needham. 1988. Attraction between lipid bilayer membranes in concentrated solutions of nonadsorbing polymers: comparison of mean-field theory with measurements of adhesion energy. *Macromolecules* 21:1822-1831.
50. Evans, E., and M. Metcalfe. 1984. Free energy potential for aggregation of mixed phosphatidylcholine/phosphatidylserine lipid vesicles in glucose polymer (dextran) solutions. *Biophys J* 45:715-720.
51. Kozlov, M. M., and V. S. Markin. 1983. Possible mechanism of membrane fusion. *Biophysics* 28:255-261.
52. Evans, E., V. Heinrich, F. Ludwig, and W. Rawicz. 2003. Dynamic tension spectroscopy and strength of biomembranes. *Biophys J* 85:2342-2350.
53. Karatekin, E., O. Sandre, H. Guitouni, N. Borghi, P. H. Puech, and F. Brochard-Wyart. 2003. Cascades of transient pores in giant vesicles: line tension and transport. *Biophys J* 84:1734-1749.
54. Tamba, Y., and M. Yamazaki. 2005. Single giant unilamellar vesicle method reveals effect of antimicrobial peptide magainin 2 on membrane permeability. *Biochemistry* 44:15823-15833.

Figure Captions

Figure 1. A. Schematic of the GUV experiment. Micropipette 1 was used to inject an isotonic PEG solution toward the held GUVs. Micropipette 2 and 3 each aspirated a GUV and positioned them close to each other. The opening of micropipette 1 was 150-300 μm away from the GUVs. B. (Left) Rh-DOPE originally contained in one GUV transferred to another GUV upon hemifusion. The image was taken at 190 sec after hemifusion. (Right) Calcein contained inside one GUV did not leak out in hemifusion. The image was taken at 200 sec after hemifusion. (scale bar 20 μm)

Figure 2. A. During the injection of PEG solution (the jet of injection visible), two GUVs made of pure DOPC were attracted to each other and slightly flattened at the contact. B. As soon as the injection stopped, the GUVs bounced back. (scale bar 50 μm)

Figure 3. Three cases of hemifusion. The lipid fluorescence dye was seen transferred from one to another which originally had no dye. A. GUVs of DOPC/DOPE/cholesterol in 8/0/2. B. GUVs of 5/5/0. C. GUVs of 4/4/2. (A weak white light was used to monitor the positions of micropipettes; scale bar 50 μm)

Figure 4. Success rate of hemifusion for four different lipid compositions in the molar ratios of DOPC/DOPE/cholesterol. One run for DOPC was counted as hemifusion because a slight lipid dye transfer was observed (see Figure 5).

Figure 5. The fluorescence intensity I of Rh-DOPE transferred to the GUV originally contained no dye, normalized by the fluorescence intensity I_0 of the GUV originally contained the lipid dye, as a function of time. $t = 0$ was the moment the GUVs attached to each other. The injection of PEG solution was stopped either at $t = 0$ or a few seconds later. The examples shown here were selected from those with long observation time (>5 minutes). The data for DOPC is an exceptional case; no other runs of DOPC showed any dye transfer.

Figure 6. Configuration of hemifusion. The image is from Figure 3C as an example. The configuration is defined by the radius R and the flattened height h . (scale bar 20 μm)

Figure 7. Phase diagram of the four lipid composition at 25° C. The symbols are L for the lamellar phase, R for the rhombohedral phase and H for the inverted hexagonal phase detected by X-ray diffraction (46, 47). L/H and R/H indicate coexisting phases. Previously at 35° C pure DOPC was found to transform from the L phase to the R phase below 44% RH (46). At 25° C the transition RH should be lower than 44% (46).

Figure 1

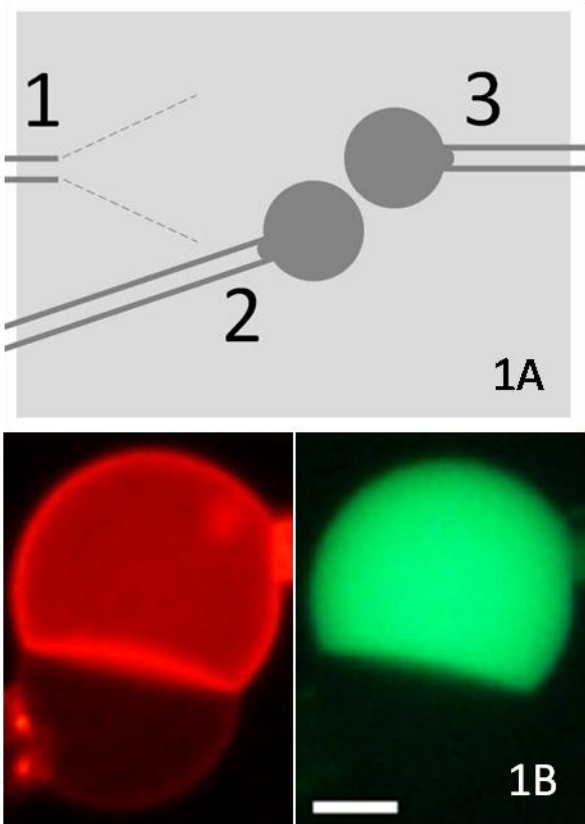


Figure 2

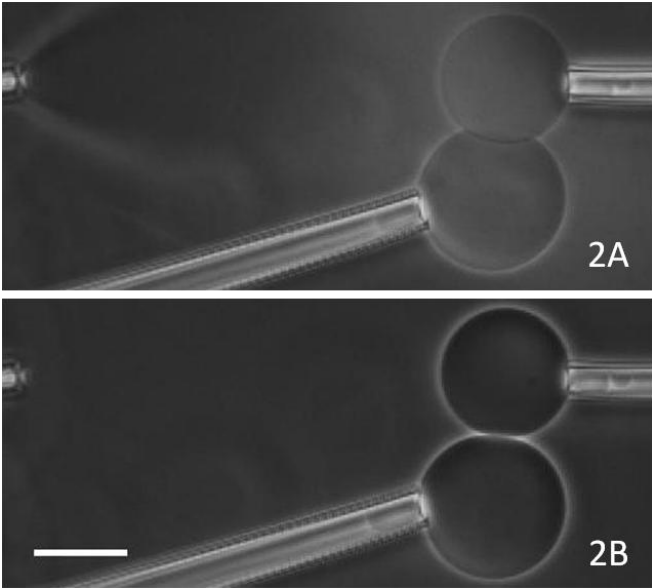


Figure 3

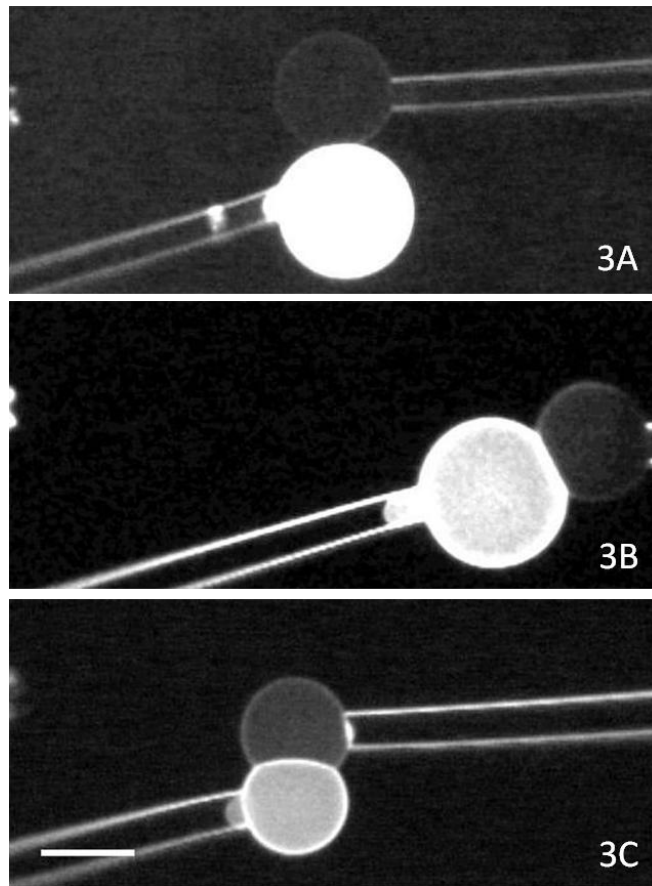


Figure 4

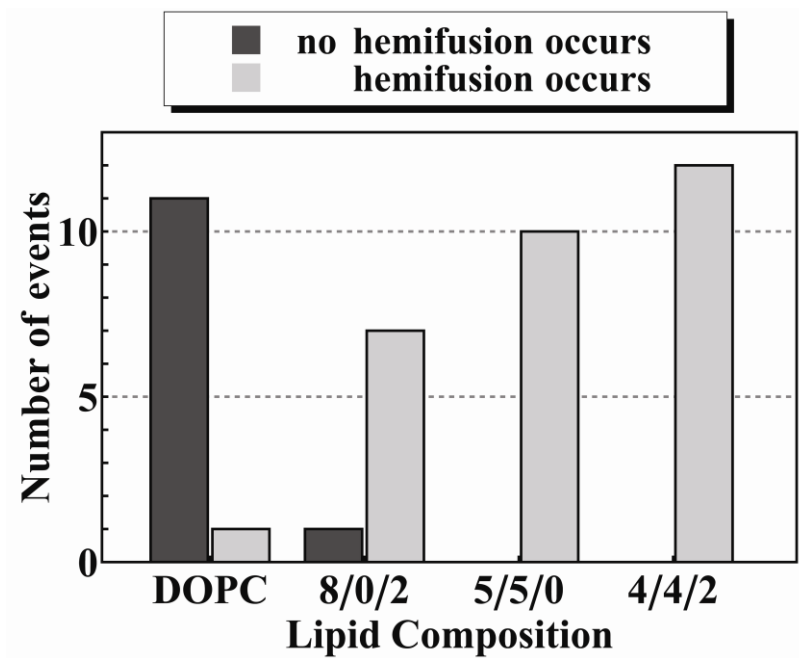


Figure 5

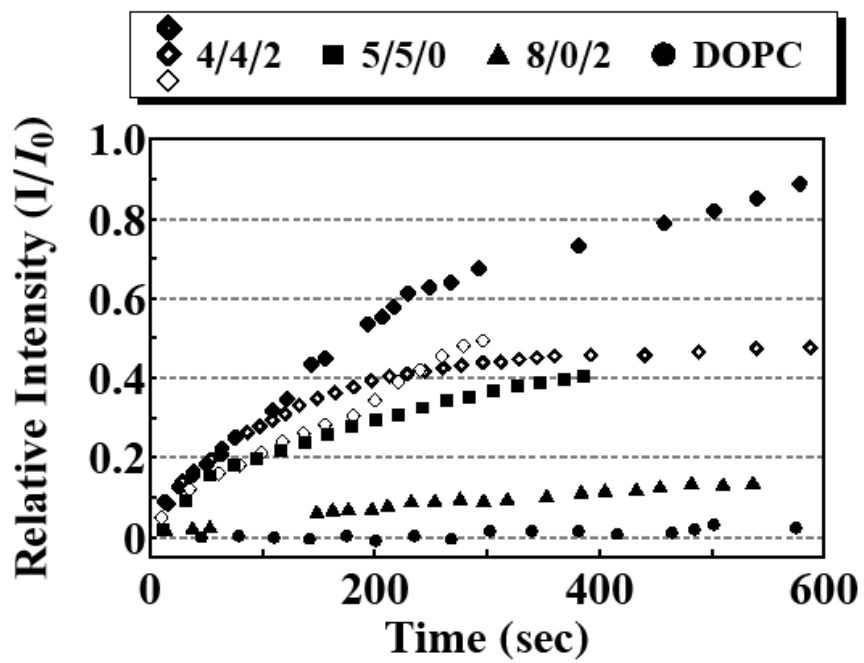


Figure 6

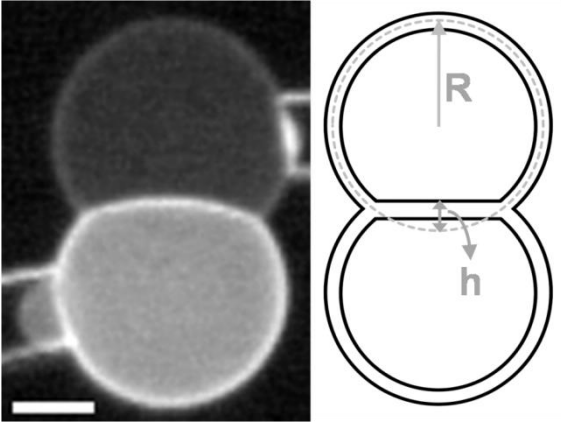


Figure 7

